



# Visible light emissions during flash sintering of 3YSZ are thermal radiation

Christian Bechteler<sup>\*</sup>, Andrew Kirkpatrick, Richard I Todd

University of Oxford, Department of Materials, Parks Road, Oxford OX1 3PH, UK

## ARTICLE INFO

### Keywords:

Flash sintering  
Black body radiation  
Thermal radiation  
Optical spectroscopy  
Joule heating

## ABSTRACT

Flash sintering enables the densification of ceramics at low furnace temperatures in a few seconds by the application of an electric field to the specimen. One of the earliest mechanisms proposed to explain the rapid densification involves the generation of Frenkel defects. Light emission during flash sintering is often interpreted as electroluminescence from electron-hole pair recombination, in support of this mechanism. In this work, experimental investigation of the emissions during flash sintering of the most widely studied ceramic, 3YSZ, shows that the visible spectrum can be explained completely in terms of black body (thermal) radiation resulting from the Joule heating of the specimen rather than electroluminescence. Apparent peaks in the spectrum are experimental artefacts associated with the equipment. There is no evidence in the visible emission spectrum during flash sintering of 3YSZ for electron-hole pair recombination associated with Frenkel pair formation or for any mechanism other than Joule heating.

Flash sintering (FS) involves the application of electrical fields during the densification of ceramic materials. The great advantage of FS is the possibility of densifying ceramics at low furnace temperatures in a very short time and it is therefore a promising and sustainable sintering technology.

Several mechanisms which might be responsible for the rapid densification have been discussed in the literature. One of the earliest proposals was that the applied electric field generates an avalanche of Frenkel defects that ionize into highly mobile, charge-neutral vacancies and interstitials and electron-hole pairs [1]. However, numerous objections have been raised to this proposal. One is that the thermal and electrical characteristics of flash sintering can be completely explained in terms of the thermal runaway of Joule heating [2,3] resulting from the combined effect of the inherent negative temperature coefficient of resistivity of most ceramics under the conditions of FS, the increase in conductivity caused by the early stages of sintering and electrochemical reduction that occurs in some ceramics when using direct currents. Many papers have now corroborated this [4–6] so it is not necessary to invoke avalanches of Frenkel defects to explain this aspect of FS.

Similarly, the rapid densification seems to be primarily a consequence of the rapid heating in FS rather than a direct effect of the electric field, as densification on similar timescales has been achieved by heating powder compacts at similar rates to those experienced during FS but without using the passage of an electric current through the specimen as the heat source [7–9]. Again, whatever the detailed mechanism

responsible for the effect of rapid heating, it is not consistent with the field-induced generation of Frenkel defects.

More direct evidence against the formation of Frenkel defects as an important mechanism in FS of ionic conductors has been presented by Schie and co-workers, who investigated the field strength necessary for their formation. The conclusion was that field strengths of  $\sim 10 \text{ GV m}^{-1}$  are necessary for the formation of Frenkel defects in ionic conductors such as zirconia [10], which is six orders of magnitude greater than the fields typically used in flash sintering.

Despite these objections, the Frenkel defect mechanism is still sometimes mentioned as a potential mechanism for FS. A key observation cited in its support and often regarded as a distinctive signature of FS is the fact that specimens emit light during the process [11–13]. This has been interpreted as electroluminescence resulting from the recombination of the electron-hole pairs created during the ionization of the Frenkel defects, although other possible mechanisms based on more established defect reactions have also been proposed [14,15].

There are, however, several unanswered questions concerning these experimental observations. First, although [11] and [12] both concern flash sintering of 3YSZ from the same powder, the primary peaks identified are at markedly different wavelengths (740 nm in [11], 1175 nm in [12]). Secondly, although it is argued that the observed spectra do not conform to the expectation from black body (thermal) radiation, no explanation is given as to why this source of radiation is apparently absent.

<sup>\*</sup> Corresponding author.

E-mail address: [Christian.Bechteler@Wolfson.ox.ac.uk](mailto:Christian.Bechteler@Wolfson.ox.ac.uk) (C. Bechteler).

<https://doi.org/10.1016/j.scriptamat.2022.114849>

Received 23 April 2022; Received in revised form 24 May 2022; Accepted 30 May 2022

Available online 8 June 2022

1359-6462/© 2022 The Authors. Published by Elsevier Ltd on behalf of Acta Materialia Inc. This is an open access article under the CC BY license (<http://creativecommons.org/licenses/by/4.0/>).

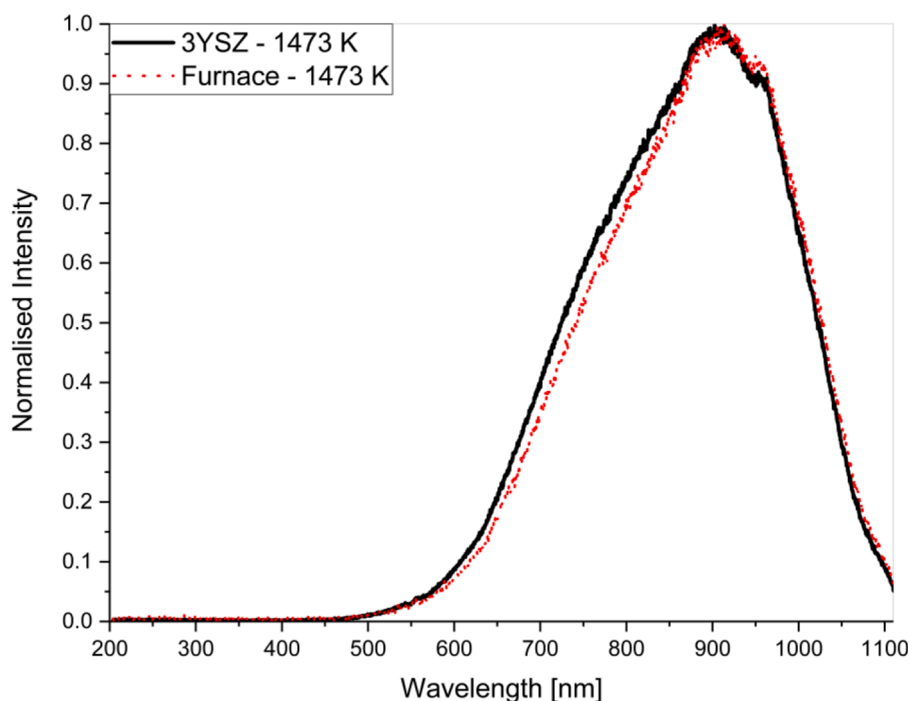


**Fig. 1.** Measured spectrum of the 1473 K graphite-furnace and the spectrum of 3YSZ in the constant current/power stage at an estimated temperature of 1473 K.

A more detailed study of the emission of light during FS of alumina has been published by Biesuz and co-workers [15]. In contrast to Raj and co-workers [11–13], these authors were able to explain their spectra mainly in terms of thermal emission. Although a few features were identified in the spectrum that were not explained as thermal radiation, they found nothing that could be attributed to electroluminescent phenomena or intrinsic luminescence. [15]

It is important to resolve the apparent contradiction between the reported results and interpretations concerning the emission of light during FS, not just to ascertain the cause of the phenomenon itself but also to test the association of the light emissions with the Frenkel defect theory. This paper investigates the issue using carefully controlled experiments to characterise the effect of the equipment used on the emission spectra and to extend similar analysis methods to those used by Biesuz et al. on alumina [15] to 3YSZ, the ionic conductor most used by Raj and co-workers both to investigate the light emissions [11,12] and in the justification of the Frenkel defect avalanche hypothesis as an explanation for FS [16].

The samples for the experiments were prepared from 3YSZ powders (TZ-3YB-E, Tosoh, Japan). These were uniaxially pressed into bars which were then cold isostatically pressed before pre-sintering at 1350°C for 5 h. This resulted in nearly fully densified samples, exceeding 98% relative density, with dimensions of  $20 \times 1.7 \times 4.6 \text{ mm}^3$ .

Platinum paste and wires were used to connect the samples to a DC power supply (EA-PSI 9750-60; EA Elektro-Automatik GmbH & CO. KG, Germany). FS-experiments were executed in an alumina tube furnace at a constant temperature of 800°C in air. At the beginning of each FS-experiment the power supply was operated under voltage control (150 V/cm) and then switched to power control at the point when a pre-defined power dissipation in the sample was achieved. The sample temperature was estimated based on the power using the black body model [16]. 0.7 was used as surface emissivity [17]. Emitted light was collected in the power-controlled quasi-steady state stage, often described as the third stage of FS.

Additional experiments, which simulate a black body, were conducted to determine the influence of the complete spectroscopic measurement system (fused silica lens, fibre, spectrometer) on the detected spectra. These experiments were executed by covering the inside of the

alumina tube in the furnace with carbon foil and inserting a piece of graphite in the hot region of the furnace. This setup is referred to as “graphite-furnace” below.

Light from the furnace and sample was collected by a 2” fused silica Achromatic doublet lens ( $f=280\text{mm}$ ) which imaged the sample to a fibre coupled spectrometer. The components were aligned to focus 400–550 nm light on the fibre, which is below the wavelengths at which most light was emitted during the experiments. The fibre couple acted as a spatial filter to remove the out of focus thermal radiation preventing damage to the fibre and reducing the influence of the collection system on the relative intensity at higher wavelengths. Most of the experiments used a QP400-2-VIS-BX fibre but a QP400-2-SR-BX fibre was also used to investigate the effect of the fibre on the spectra obtained. The recorded spectra were evaluated using OceanView software.

Two lasers with wavelengths of 520 nm and 532 nm were used to check the wavelength calibration of the spectrometer (OceanOptics HDX, range 200 - 1120 nm). This showed the measurement of the wavelength was accurate to within 0.6 nm.

An integration time of 6 ms was used throughout. The detection efficiency of the spectrometer was determined using a known light source (Sylvania Satin 40W 240V) with a colour temperature of 2700 K, without the fused silica lens and fibre.

Theoretical black body spectra were calculated for comparison with the experimental results using Planck’s Law. These are referred to as “calculated” spectra in what follows.

**Fig. 1** compares the detected spectra of 3YSZ during FS and the graphite-furnace measurement for a nominal temperature of 1473 K. The temperature was achieved using the black body model estimation of the FS sample temperature for the 3YSZ and the thermocouple reading of the furnace for the simulated black body. Both spectra were normalised to 1 at their maximum intensity.

It is evident that the spectra are very similar and there are no additional emission peaks in the YSZ although the spectra are not exactly overlapping at all wavelengths. Furthermore, both spectra display a dip at  $\sim 950 \text{ nm}$  and the maximum intensity is located at  $\sim 900 \text{ nm}$  in both cases, whereas according to Wien’s displacement law, the maximum black-body intensity at 1473 K should be at approximately 1970 nm. To detect possible explanations for the shape and the origin of the spectra,

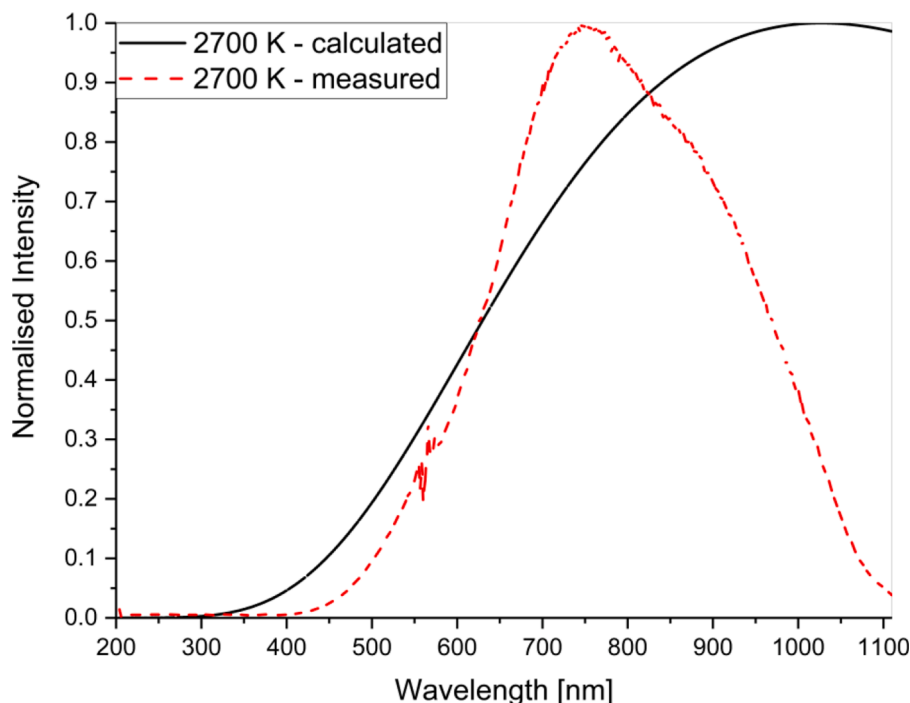


Fig. 2. Measured spectrum of the 2700 K lamp without additional lens or fibre and the calculated spectrum referring to Planck's law at the same temperature.

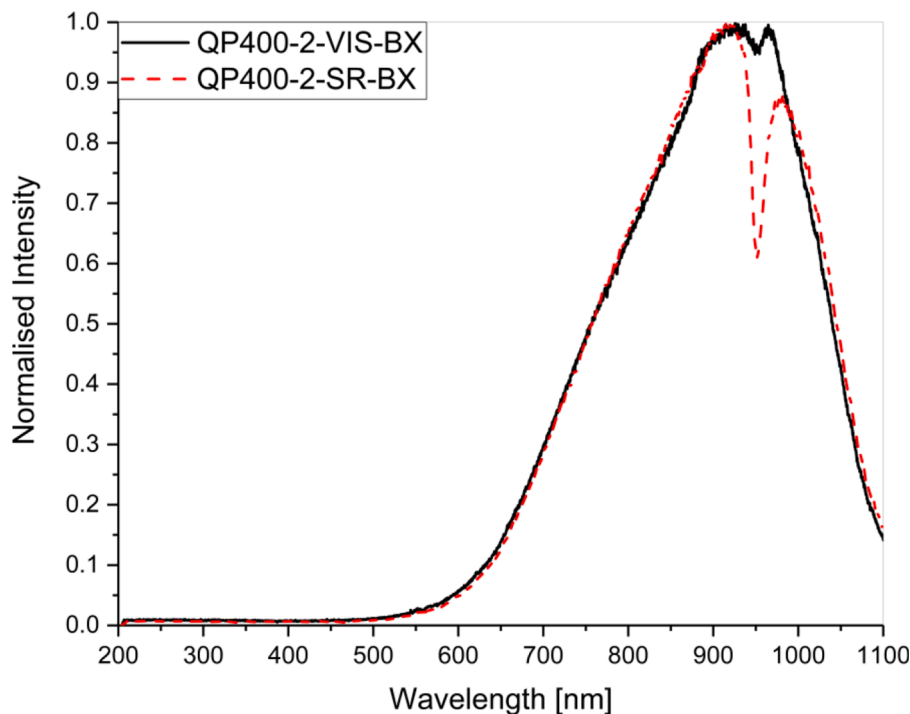


Fig. 3. Furnace spectrum measured with two different fibres under same conditions and without any other changes.

further measurements and calculations were conducted.

To determine the influence of the spectrometer itself, without the focusing lens and fibre, the emitted spectrum of the 2700 K lamp was measured and compared with the calculated spectrum for the same temperature (Fig. 2), normalising the spectra with respect to the maximum intensity as above.

As in Fig. 1, the experimental curve shows a strongly decreasing intensity at higher wavelengths, well before the calculated maximum intensity ( $\sim 1050$  nm). Furthermore, there is an abnormal deviation of the expected behaviour at approximately 550 nm. Based on Fig. 2 it can

be assumed that the spectrometer causes two main issues. First, strongly decreasing detection efficiency at higher wavelengths which leads to a shifted peak intensity. Second, an artefact around 550 nm, which causes a local oscillation in intensity. This is not noticeable in the results below because most of the intensity is at higher wavelengths owing to the lower temperatures involved.

Fig. 3 shows graphite-furnace spectra at 1273 K measured with two different fibres. The dip at 950 nm detected in Fig. 1 is evident for both fibres but is in the form of a very strong minimum for the QP400-2-SR-BX fibre, to the extent that it leads to apparent peaks in intensity on

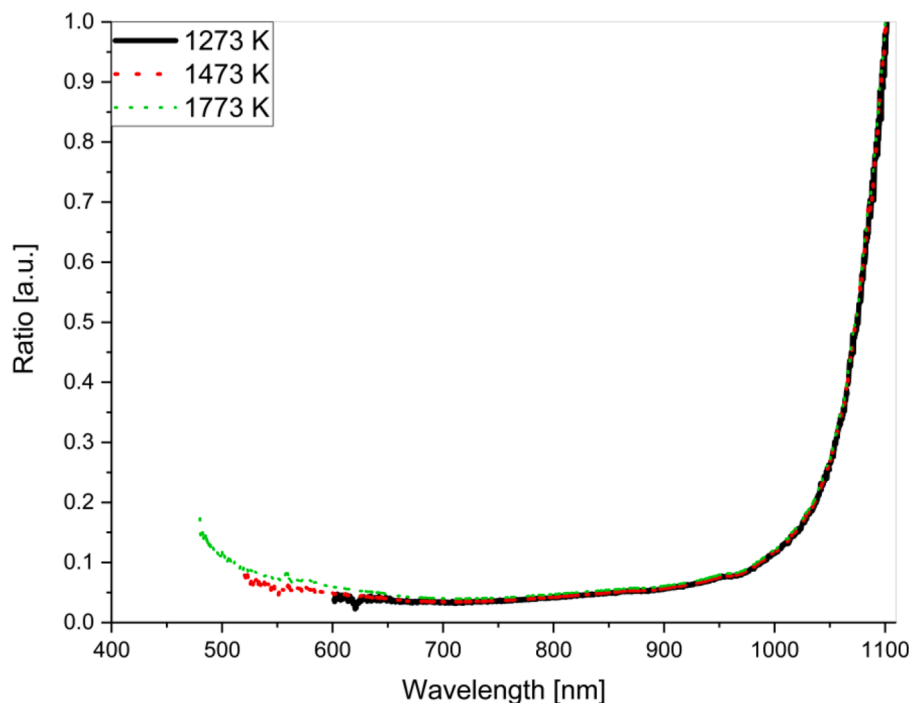


**Fig. 4.** Calculated ratio between calculated BBR and the measured spectrum at varying temperatures. The undulations at low wavelengths are noise due to the low intensity.

either side of it. The higher attenuation of the QP400-2-SR-BX fibre, compared to the QP400-2-VIS-BX, at around 950 nm is evident in the manufacturer's specification, as shown in Fig. S1 in the supplementary information. Absorption at this wavelength is associated with  $\text{OH}^-$  ions in the fibre [18].

It is emphasised that Fig. 3 is the result from the graphite-furnace alone. Inspection of the “peaks” identified previously in the emission spectra of flash sintering 3YSZ [3,4] shows that they can also be interpreted as being a consequence of minima superimposed on a broader

spectrum representing black body radiation (BBR), truncated at higher wavelengths in the case of reference [3] and the present work by the reduction in efficiency of the spectrometer. The electroluminescence “peak” identified in [11] is immediately below the minimum, at 740 nm whereas the corresponding feature in Fig. 3 is at 920 nm; there is no fluctuation in the spectrum around 740 nm in this work. It seems highly probable that the significantly different positions of the “peaks” in [11, 12] and the present work arise because they are an artefact of the collection system (spectrometer and collection optics), which was

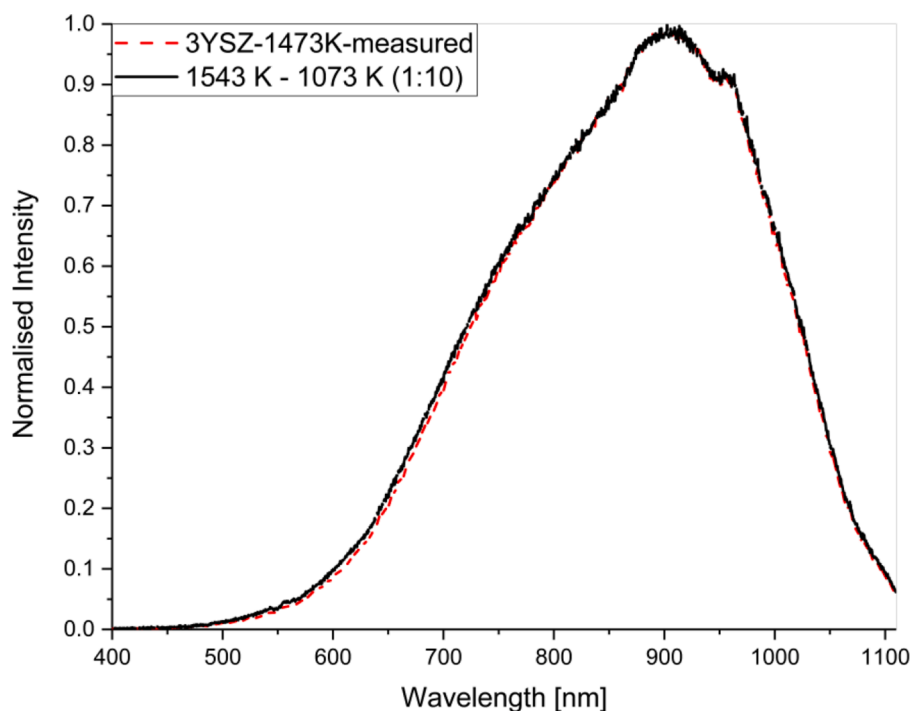


**Fig. 5.** Measured 3YSZ spectrum and recalculated spectrum for a (sample-)temperature of 1543 K including background radiation at 1073 K at an estimated ratio of 1:10.

different in the three papers. No control experiments without the flash sintering specimen are reported in [11,12] and the wavelength limit of our system prevents direct comparison with the results in [12].

In order finally to rule out any significant electroemission in the wavelength range investigated, we now return to the small discrepancies between the spectra of the graphite-furnace and the flash sintering 3YSZ specimen in Fig. 1. In order to investigate these, the ratio between the calculated BBR intensity and the result from the graphite-furnace, which can be seen as an approximation to a black body, was calculated for three different experimental temperatures (1273, 1473 and 1773 K). These ratios are shown as a function of wavelength in Fig. 4. All ratios were normalised to 1 at 1100 nm. The results show that the ratio is independent of temperature. Fig. 4 can therefore be used in conjunction with Planck's law to predict the spectrum that would be measured experimentally for any temperature.

We use this here to demonstrate that the minor discrepancies in Fig. 1 can be explained as a consequence of the non-uniformity of the temperature in and around the flash sintering specimen. There are two main sources of non-uniformity. The first is that although the black body model used to estimate the specimen temperature assumes a uniform surface temperature, in reality the temperature is non-uniform, being hotter towards the centre-line of the specimen [19]. Recent modelling shows that the maximum surface temperature for similar specimens may exceed the mean surface temperature by  $\sim 70$  K [20]. The second source of non-uniformity is that although BBR from the flash sintering 3YSZ specimen is much more intense than that from the furnace at 1073 K, it accounts for only a small fraction of the area sampled by the spectrometer ( $\sim 10\%$  of the furnace cross section) so the contribution of the furnace to the total intensity may not be negligible. These factors can change the form of the spectrum.

A full calculation of the effects of the non-uniform temperature would require detailed modelling of the specimen surface temperature and would also be susceptible to the uncertainty in emissivity for such specimens (which is itself a function of wavelength [21]). However, the simple approximation of combining the extremes of the temperature distribution in ratios appropriate to their cross-sections demonstrates that the range of temperatures present provides a convincing explanation of the experimental temperature distribution during flash sintering in Fig. 1. Fig. 5 shows the response predicted using Planck's law and the measuring system response curve in Fig. 4 for a simulated experiment consisting of a specimen at a temperature of 1543 K (i.e. a maximum surface temperature 70 K hotter than the uniform temperature estimate of 1473 K in Fig. 1) plus a furnace background at 1073 K, the latter contribution being added in at 10 times the former to account for the larger area of the furnace background compared with the specimen. It can be seen that the predicted response matches the experimental flash sintering spectrum almost perfectly.

We conclude that the observed spectrum of flash sintering 3YSZ specimens in the range 400–1100 nm, which includes the vast majority of the visible spectrum, can be completely explained solely in terms of black body radiation and the influence of the experimental detection system. As in alumina [6], there is no evidence to support the existence of electroluminescence in the visible spectrum during flash sintering of 3YSZ from electron-hole pair recombination due to Frenkel defect formation or any other source.

In closing, we note that this does not rule out emissions from 3YSZ in other regions of the spectrum nor from other ceramics in the visible part of the spectrum. Indeed, it would not be surprising if such emissions do exist, particularly in YSZ. Departures from black-body behaviour in the infrared spectrum of the zirconia-based Nernst glower were noted by Coblenz as early as 1908 [22] YSZ is also well known to luminesce under a variety of conditions [23,24]. Most relevantly, flash sintered 3YSZ exhibits blue photoluminescence at room temperature that does not occur with conventionally sintered material [25]. However, these emissions are weak compared with the very bright visible emissions

during flash sintering of 3YSZ, which this paper has shown to be black body radiation. This is the consequence of the high specimen temperature caused by Joule heating during flash sintering.

In summary, the light emission from 3YSZ during flash sintering can be completely explained in terms of black body (thermal) radiation resulting from Joule heating of the specimen. Apparent peaks in the visible spectrum reported previously are artefacts of the experimental equipment such as absorption by the optical fibre. There is no evidence in the visible emission spectrum from flash sintering of 3YSZ for electroluminescence caused by electron-hole pair recombination due to Frenkel pair formation or any other source.

## Declaration of Competing Interest

The authors declare that they have no known competing financial interests or personal relationships that could have appeared to influence the work reported in this paper.

## Acknowledgements

The authors would like to thank Ocean Insight and Callum Ross for the use of the spectrometer and useful discussions.

## Funding

This work was supported by the Engineering and Physical Sciences Research Council [EP/T517811/1].

## Supplementary materials

Supplementary material associated with this article can be found, in the online version, at doi:[10.1016/j.scriptamat.2022.114849](https://doi.org/10.1016/j.scriptamat.2022.114849).

## References

- [1] R. Raj, M. Cologna, J.S.C. Francis, *J. Am. Ceram. Soc.* 94 (2011) 1941–1965.
- [2] R.I. Todd, E. Zapata-Solvas, R.S. Bonilla, T. Sneddon, P.R. Wilshaw, *J. Eur. Ceram. Soc.* 35 (2015) 1865–1877.
- [3] Y. Zhang, J.-I. Jung, J. Luo, *Acta Mater.* 94 (2015) 87–100.
- [4] E. Bichaud, J.M. Chaix, C. Carry, M. Kleitz, M.C. Steil, *J. Eur. Ceram. Soc.* 35 (2015) 2587–2592.
- [5] J.G.P. Da Silva, H.A. Al-Qureshi, F. Keil, R. Janssen, *J. Eur. Ceram. Soc.* 36 (2016) 1261–1267.
- [6] M. Biesuz, V.M. Sglavo, *J. Eur. Ceram. Soc.* 36 (2016) 2535–2542.
- [7] W. Ji, B. Parker, S. Falco, J.Y. Zhang, Z.Y. Fu, R.I. Todd, *J. Eur. Ceram. Soc.* 37 (2017) 2547–2551.
- [8] W. Ji, J. Zhang, W. Wang, Z. Fu, R.I. Todd, *J. Eur. Ceram. Soc.* 40 (2020) 5829–5836.
- [9] Y. Zhang, J. NIE, J.M. Chan, J. Luo, *Acta Mater.* 125 (2017) 465–475.
- [10] M. Schie, S. Menzel, J. Robertson, R. Waser, R.A. de Souza, *Phys. Rev. Materials* 2 (2018).
- [11] J.-M. Lebrun, R. Raj, *J. Am. Ceram. Soc.* 97 (2014) 2427–2430.
- [12] K. Terauds, J.-M. Lebrun, H.-H. Lee, T.-Y. Jeon, S.-H. Lee, J.H. Je, R. Raj, *J. Eur. Ceram. Soc.* 35 (2015) 3195–3199.
- [13] K. Naik, S.K. Jha, R. Raj, *Scr. Mater.* 118 (2016) 1–4.
- [14] R. Kirchheim, *Solid State Ionics* 320 (2018) 239–258.
- [15] M. Biesuz, P. Luchi, A. Quaranta, A. Martucci, V.M. Sglavo, *J. Eur. Ceram. Soc.* 37 (2017) 3125–3130.
- [16] R. Raj, *J. Eur. Ceram. Soc.* 32 (2012) 2293–2301.
- [17] H. Tanaka, S. Sawai, K. Morimoto, K. Hisano, *J. Therm. Anal. Calorim.* 64 (2001) 867–872.
- [18] M. Ding, D. Fan, W. Wang, Y. Luo, G.-D. Peng, in: G.-D. Peng (Ed.), *Handbook of Optical Fibers*, Springer, Singapore, 2019, pp. 1–39.
- [19] M. Yoshida, S. Falco, R.I. Todd, *J. Ceram. Soc. Japan* 126 (2018) 579–590.
- [20] Y. Li, R. Torchio, S. Falco, P. Alotto, Z. Huang, R.I. Todd, *J. Eur. Ceram. Soc.* 41 (2021) 6649–6659.
- [21] S.M. Avdoshenko, A. Strachan, *Modell. Simul. Mater. Sci. Eng.* 22 (2014) 75004.
- [22] W.W. Coblenz, *bull. Natl. Bur. Stand.* 4 (1908) 533.
- [23] J.-M. Costantini, F. Beuneu, M. Fasoli, A. Galli, A. Vedda, M. Martini, *J. Phys.* 23 (2011), 115901.
- [24] K. Wang, L. Ma, X. Xu, S. Wen, Y. Zhang, *Langmuir ACS J. Surf. Colloids* 31 (2015) 8224–8227.
- [25] Y. Yamashita, T. Kurachi, T. Tokunaga, H. Yoshida, T. Yamamoto, *J. Eur. Ceram. Soc.* 40 (2020) 2072–2076.